Growth and characterization of TbAs:GaAs nanocomposites

Laura E. Cassels[a)]
Department of Materials Science and Engineering, University of Delaware, Newark, Delaware 19711

Trevor E. Buehl, Peter G. Burke, Chris J. Palmstrøm, and Art C. Gossard
Materials Department, University of California–Santa Barbara, Santa Barbara, California 93106

Gilles Pernot and Ali Shakouri
Electrical Engineering Department, University of California–Santa Cruz, Santa Cruz, California 95064

Chelsea R. Haughn, Matthew F. Doty, and Joshua M. O. Zide
Department of Materials Science and Engineering, University of Delaware, Newark, Delaware 19711

(Received 28 October 2010; accepted 25 January 2011; published 28 February 2011)

Recently, there has been interest in semimetallic rare earth monopnictide nanoparticles epitaxially embedded in III-V semiconductors due to the drastic changes brought about in these materials' electrical and thermal properties. The properties of terbium codeposited with gallium arsenide by molecular beam epitaxy are discussed here. These new materials were characterized by x-ray diffraction, Rutherford backscattering spectrometry, resistivity measurements, photoluminescence, time-domain thermoreflectance thermal conductivity measurements, optical absorption spectroscopy, and plan-view high-angle annular dark-field scanning transmission electron microscopy. Results revealed successful formation of randomly distributed nanoparticles with an average diameter of ~1.5 nm, reduction of thermal conductivity by a factor of about 5, and consistency with theoretical predictions of mid-band-gap Fermi level pinning and behavior of past similar materials. The success of these TbAs:GaAs materials will lead the way for growth of similar materials [TbAs:InGa(Al)As] which are expected to exhibit highly desirable thermoelectric properties. [DOI: 10.1116/1.3555388]

I. INTRODUCTION

Semimetallic rare earth monopnictide nanoparticles epitaxially deposited within III-V semiconductors have been shown to cause radical changes in the electrical and thermal transport properties of the resulting composite materials.[1] Indeed, ErAs and ErSb nanoparticles have modified GaAs, GaSb, InGa(Al)Sb, and InGa(Al)As semiconductors, donating carriers,[2] pinning Fermi levels,[2] reducing carrier lifetimes,[3] scattering phonons,[4,5] and enhancing electron tunneling efficiency, depending on the matrix.[6] Thermoelectric (TE) materials are one of many applications of this type of composite system. Based on the effects of nanoparticle formation in these Er-containing systems and their success as TE materials,[1,5] related terbium arsenide/III-V nanocomposite systems are likely to behave similarly. Here, TbAs was codeposited with GaAs by molecular beam epitaxy (MBE) with the goal of characterizing these materials to understand the potential of TbAs nanoparticles for improving TE conversion efficiency in other III-V semiconductors.

TE devices are used for either generating power (the Seebeck effect) or for localized heating and cooling (the Peltier effect). The dimensionless TE figure of merit, ZT, is a measure of a material's ability to extract power from a temperature gradient and vice versa, where a higher ZT translates to higher device efficiency. ZT is given by $ZT=S^2\sigma T/\kappa$, where S is the Seebeck coefficient ($\Delta V/\Delta T$ in a thermal gradient), σ is the electrical conductivity, and κ is the thermal conductivity.[7] Although electrical and thermal properties are naturally intertwined, epitaxial growth methods allow new materials to be engineered which aim to partially decouple these parameters. In the case of ErAs:InGa(Al)As and ErSb:InGa(Al)Sb, nanoparticles improve ZT relative to the matrix by reducing thermal conductivity (through phonon scattering), increasing Seebeck coefficient (through electron filtering or energy-dependent electron scattering), and increasing electrical conductivity (through nanoparticle donation of electrons).[5,8]

TbAs nanoparticles are expected to behave similarly to ErAs nanoparticles yet ultimately lead to a higher ZT due to their different lattice mismatches to relevant III-V semiconductors. Much like ErAs, TbAs nanoparticles are expected to be semimetallic but have a larger lattice constant of 5.824 Å.[9] It has been shown that strain can be used to shift the Fermi level of such nanocomposite materials away from a universal donor level.[2,10–12] Since the strain states of TbAs in these III-V semiconductors vary from those of ErAs, it is anticipated that the Fermi levels of TbAs-containing III-V's will be shifted to slightly different positions as a result. Indeed, tensile strain caused by the nanoparticles is expected to shift the Fermi level of the matrix up in energy from a universal donor level, while compressive strain is expected to shift the Fermi level of the matrix down from the universal donor level, toward the valence band.[11] This has led to the estimation that the small tensile strain of TbAs in InGaAs ($<1\%$) will pin the Fermi level of TbAs:InGaAs near the conduction band edge, and the ~3% compressive strain of

a)Electronic mail: lcassels@udel.edu

TbAs in GaAs is predicted to pin the Fermi level near midgap. Although this would render TbAs:GaAs a poor TE material, this largely unexplored class of materials may open doors for a variety of other applications, and these samples are therefore useful for determining the structural, electrical, and thermal changes that TbAs nanoparticles will bring about in other III-V semiconductors. Even though very little has been published about TbAs, it is expected that the slight differences in electronic configuration between terbium and erbium (only tightly bound *f*-shell electrons) will not cause a major difference in electronic properties,[11] allowing strain effects in the nanocomposites to dominate. Indeed, the electrical resistivity of bulk TbAs has been measured to be 1.8×10^{-3} Ω cm (vs 7.2×10^{-3} Ω cm for ErAs), and its Seebeck coefficient is +18 μV/°C (vs +16 μV/°C for ErAs), consistent with a semimetal.[13]

II. EXPERIMENT

The TbAs:GaAs materials were grown by MBE and characterized by several techniques including x-ray diffraction (XRD), Rutherford backscattering spectrometry (RBS), resistivity measurements, photoluminescence (PL), time-domain thermoreflectance (TDTR), optical absorption spectroscopy (OAS), and plan-view high-angle annular dark-field scanning transmission electron microscopy (HAADF STEM).

A. Growth of materials by MBE

The two TbAs:GaAs samples presented here were grown with an OSEMI NextGEN solid-source MBE system. All growth conditions were identical for both samples with the exception of the terbium source temperature. The terbium source was an E-Science high temperature effusion cell with a conical tungsten crucible. At a substrate temperature of 490 °C (as measured by band-edge thermometry), terbium was codeposited with gallium and arsenic such that the solid solubility limit of Tb in GaAs was exceeded, and nanoparticles precipitated randomly throughout the material. This precipitation was previously shown to occur in the case of GaAs and InGaAs codeposited with erbium.[5,14] A GaAs growth rate of 1 μm/h was used for an expected film thickness of 1 μm on undoped (001) GaAs wafers with a 50 nm undoped GaAs buffer layer. No capping layers were grown. An arsenic-to-gallium flux ratio of about 100:1 was used. Lastly, the growth and thermal desorption of oxides were monitored with reflection high-energy electron diffraction (RHEED). RHEED patterns signified three-dimensional (3D) growth, similar to the patterns we observed in high-concentration ErAs:III-V growths.[15]

It has proven very difficult to measure the flux of Tb from beam equivalent pressure measurements. We speculate that the cause of the flux measurement problem is the low vapor pressure of Tb at the temperature of the filament of the beam flux monitor ion gauge, causing Tb to stick to the filament and preventing accurate flux measurements. Because of this challenge, TbAs concentration was initially calibrated from lattice constant dilation by terbium atoms in the materials as measured by XRD as a function of Tb effusion cell temperature. It was later revealed by RBS that actual concentrations were much lower than expected due to superdilation of the lattice constant (will be discussed later). For the two samples grown in this paper, Tb source temperatures used were 1320 and 1345 °C.

B. Sample characterization

Each of the TbAs:GaAs samples were characterized to determine room temperature structural, electronic, and thermal properties. Structural information, including the lattice constant, thickness, TbAs concentration, and qualitative degree of crystallinity, was obtained by XRD using a high-resolution PANalytical X'Pert PRO materials research diffractometer. ω-2θ rocking curves were taken around the GaAs (004) reflection in a triple crystal configuration [the first crystal being a four-bounce Ge (220) monochromator and the third a three-bounce Ge (220) analyzer crystal]. The x-ray source was the 1.54 Å wavelength $K\alpha_1$ emission line of Cu. Thickness and TbAs concentration results gathered from XRD were later compared with RBS. RBS analysis was performed at the Rutgers University Tandem Accelerator using 2 MeV He^{++} ions in a vacuum chamber at a pressure of $\sim 10^{-6}$ torr. A typical Si surface-barrier detector with an energy resolution of about 17 keV was placed at a 163° scattering angle. Ion beam current on the sample was 10–20 nA, and the beam spot was about 2 mm in diameter. Data were collected until 10 μC of charge accumulated (10–15 min). RBS data analysis was performed using the commercial program SIMNRA.

The electrical resistivity of each sample was measured in the van der Pauw geometry where indium contacts were soldered to the corners of the material cleaved to roughly 1×1 cm squares. Current was supplied by a Keithley 2400 sourcemeter and voltage was measured with a Keithley 2000 multimeter.

PL measurements of the samples were acquired using an Acton Spectrophotometer, illuminated with a Mira 900P pulsed titanium-sapphire laser at 800 nm. PL was collected for the 1345 °C TbAs:GaAs sample as well as the back of the GaAs wafer on which the sample was grown for comparison.

Room temperature thermal conductivity was measured by TDTR. In preparation, the surface was cleaned with acetone followed by isopropyl alcohol, deionized water, and a 40 s buffered HF dip to remove any oxide. Following this cleaning, an ~50 nm layer of pure Al was deposited on the surface of the samples by e-beam evaporation. For the measurement, a femtosecond laser pulse is split into two beams for pumping and probing. The pump pulse heats the Al surface, and the delayed probe pulse measures the reflectivity of the surface as a function of time as the heat diffuses into the thin film. Cross-plane thermal conductivity is estimated by fitting the experimental thermoreflectance data with a 3D thermal model based on thermal quadrupoles. More detailed explanations have been published elsewhere.[4,16]

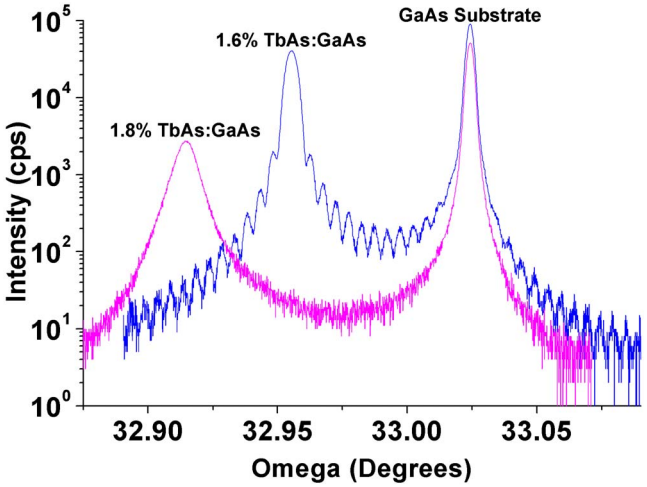

FIG. 1. (Color online) ω-2θ XRD rocking curves of two TbAs:GaAs samples found to have 1.6% and 1.8% TbAs concentrations. Fringes on the 1.6% sample were used to calculate film thickness, and the FWHMs of the film peaks indicated good crystallinity.

Optical absorption spectroscopy was performed based on interesting absorption properties found to occur in previous nanocomposite materials.[17] Spectra were obtained with a Cary 500 spectrophotometer in a range of 800–3000 nm with a 1 nm data interval. The absorption coefficient was calculated as $-\ln(T/T_0)/t$, where T is the transmission through the measured sample, T_0 is the transmission through a bare undoped GaAs substrate sample, and t is the thickness of the active TbAs:GaAs epilayer.[17]

Plan-view HAADF STEM samples were prepared by mechanical polishing without the use of Ar ion milling. A FEI Titan 80-300 STEM/TEM equipped with a field-emission electron gun operated at 300 kV was used for plan-view HAADF STEM.

III. RESULTS AND DISCUSSION

A. Structural properties

Several important observations about the structure and composition of the TbAs:GaAs samples grown were gathered from XRD and RBS. XRD spectra of the two samples grown are shown in Fig. 1. Initially, the atomic concentration of TbAs in the films was calculated from the position of the film peaks in the ω-2θ rocking curves. This was done by first calculating the lattice constant of the thin film using Bragg's law and then using Vegard's law to calculate the concentration of TbAs in the film by linear interpolation.[18] The lattice constant of TbAs was obtained from an XRD spectrum taken of a 200 nm TbAs film grown on GaAs and capped with 50 nm of GaAs. This returned a value of 5.817 Å which compares well with published values giving the lattice constant as 5.824 Å.[9] We note that the sample preparation details (including degree of crystallinity) and source material purity of previously measured TbAs materials were often not reported, making the accuracy of these measurements impossible to evaluate.[9] The concentrations of the two samples were found to be 6.6% TbAs (Tb source temperature of 1320 °C) and 10.4% TbAs (Tb source temperature of 1345 °C) by this method.

While this method initially seemed reasonable, recent data presented by Scarpulla *et al.*[19] led us to believe that the thin film lattice constants may have been dilated more than expected by Vegard's law for a given concentration, as was found in ErAs:GaAs materials at concentrations greater than 1%.[19] Following the methodology of Scarpulla *et al.*, Rutherford backscattering spectrometry was performed on the samples in order to reveal their true atomic concentrations.[19] It was found that a superdilation of lattice constant was occurring, and the actual concentrations of TbAs in the materials were $1.6\% \pm 0.05\%$ (1320 °C) and $1.8\% \pm 0.05\%$ (1345 °C). The exact cause of the superdilation is not well-known, but this phenomenon seems to occur at high levels of certain dopants in GaAs where doping is not purely substitutional, but where dopants may incorporate as precipitates, interstitials, or complexes including lattice defects such as vacancies.[20]

Additionally, thickness fringes visible in the XRD spectrum of the 1.6% TbAs sample allowed for the calculation of the actual film thickness (~0.91 μm). Film thicknesses were also calculated from RBS measurements and were in good agreement with XRD results. From RBS, the thickness of the 1.6% sample was found to be 1.00 μm and that of the 1.8% sample was found to be 1.06 μm. Finally, the narrow film peaks [full widths at half maximum (FWHMs) were 0.005° and 0.009° for the 1.6% and 1.8% samples, respectively] and thickness fringes visible indicate that the films grown were of good crystalline quality.

B. Electrical and thermal properties

No values resulted from resistivity measurements as the resistance of both of the samples was too high to measure with the equipment ($>2\times10^8$ Ω). This is consistent with predictions of a deeply pinned Fermi level in TbAs:GaAs, as described in Sec. I, where the Shockley–Hall–Reed recombination limits electron conduction severely.

The thermal conductivities of both samples were successfully measured by TDTR. The room-temperature thermal conductivity of the 1.6% TbAs sample was 17.6 ± 1.8 W/m K, while that of the 1.8% sample was 10.8 ± 1.8 W/m K. Compared to the room-temperature thermal conductivity measurement of a control sample of intrinsic GaAs, (50 W/m K, which is in reasonable agreement with published values),[21] the presence of TbAs nanoparticles in the 1.8% TbAs sample was able to reduce the thermal conductivity by around fivefold. This is quite a significant reduction and a promising result for thermoelectric materials grown in a similar manner. Furthermore, since electrical conductivity was found to be so low in these materials, the electronic contribution to the thermal conductivity is almost zero (the Wiedemann–Franz law).[22] The thermal conductance of the materials is therefore due almost entirely to phonons and the reduction in thermal conductivity can be directly attributed to the nanoparticles.

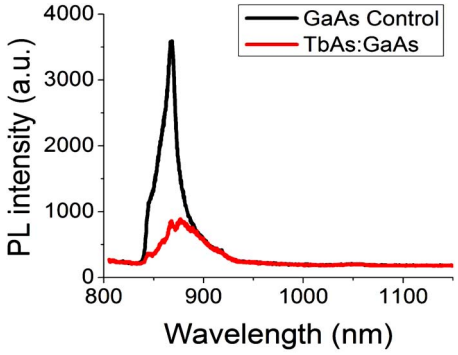

FIG. 2. (Color online) Photoluminescence signal from the 1.8% TbAs:GaAs film is quenched as seen by comparison to the spectrum of an undoped GaAs wafer.

Finally, PL measurements were performed on the 1.8% TbAs sample (Fig. 2). PL quenching was observed in comparison to a GaAs control sample (the back of the wafer), indicating that nonradiative recombination of photogenerated carriers was dominant. This signifies the existence of deep states, consistent with Fermi level predictions made in Sec. I, as well as metal-like behavior of the nanoparticles. Measurements of carrier lifetimes by optical and terahertz pump-probe techniques are ongoing but remain inconclusive so far.

C. Nanoparticle observation and characterization

The presence of nanoparticles in TbAs:GaAs was suggested by OAS and confirmed by HAADF STEM.

Both samples were first characterized with OAS [spectra are shown in Fig. 3(a)]. In each case, an absorption peak attributable to plasmon resonances was found at about 1 eV, strongly suggesting the presence of TbAs nanoparticles within the material.[17] The plasmon resonance peaks being at the same position for both concentrations suggest that the particles have similar carrier concentrations. Upon varying the angle of light polarization [Fig. 3(b)], the peak intensities and positions for both samples did not differ appreciably, suggesting possible isotropy of nanoparticle shape and distribution.

To confirm the optical absorption measurements and the existence of nanoparticles, HAADF STEM was performed on the 1.8% TbAs:GaAs sample as shown in the plan-view images in Fig. 4. Randomly distributed particles of approximately uniform size are observed. From these images, an average particle diameter of ~1.5 nm was measured. The TbAs nanoparticles exhibit the bulk TbAs rocksalt structure with a continuous As sublattice between the nanoparticles and the surrounding GaAs matrix.[15] While further examination is needed, it appears that some of the nanoparticles were slightly elongated in one of the ⟨110⟩ directions, which corresponds to the fast diffusion direction on a (001) GaAs growth surface. The average diameter of these nanoparticles was smaller than that of ErAs nanoparticles in GaAs referenced by Scarpulla *et al.*[17] (2–3 nm) but similar to those grown by Singer *et al.*[14] and Poole *et al.*[23] (1–2 nm). This can be attributed at least partially to a lower growth temperature (490 °C for this work vs 580 °C for most ErAs:GaAs growths), but other differences between terbium and erbium could also contribute to this distinction.

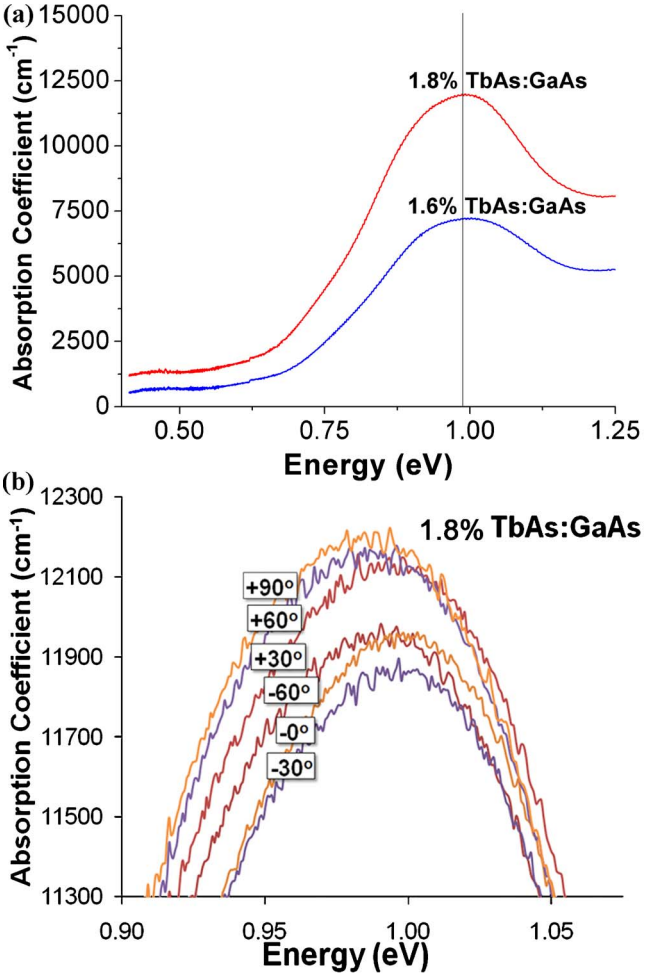

FIG. 3. (Color online) (a) Optical absorption spectra from 1.6% and 1.8% TbAs:GaAs samples showing plasmon resonance peaks near 1 eV indicating nanoparticle formation. (b) The same plasmon resonance peak is nearly invariable under different light polarizations for the 1.8% TbAs sample, signifying possible isotropy of nanoparticle shape and distribution.

IV. SUMMARY AND CONCLUSIONS

Two samples of GaAs codeposited with 1.6% and 1.8% TbAs concentrations were grown by MBE, and their electrical, thermal, and structural properties were explored. Formation of TbAs nanoparticles was confirmed through optical absorption and HAADF STEM. Moreover, high electrical resistivity and a lack of PL signal were consistent with energy band predictions and previous results in other rare earth-V/III-V nanocomposite systems.[1,2,4,5,8,17] Thermal conductivity was reduced significantly from that of the semiconductor matrix due to phonon scattering by the nanoparticles. Based on these analyses, we believe that codepositing Tb in other III-V semiconductors, particularly InGaAs and InGaAlAs, will lead to efficiency improvements in thermoelec-

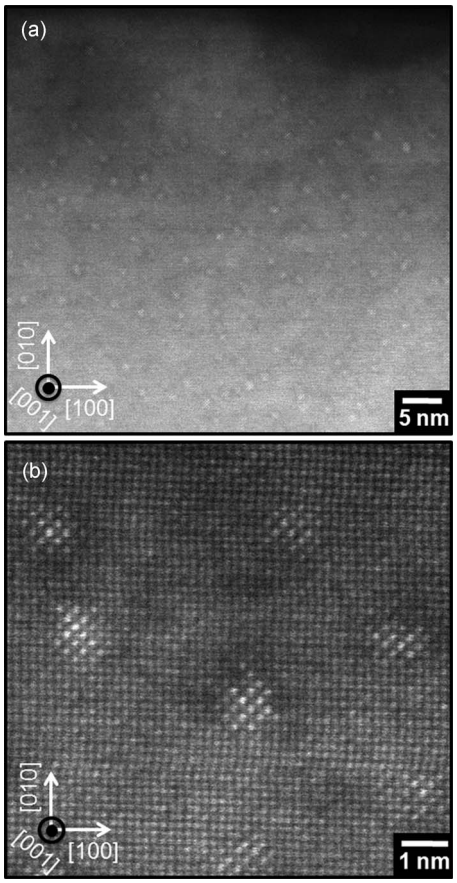

FIG. 4. (a) HAADF STEM plan-view images of self-assembled TbAs nanoparticles in GaAs grown on (001) GaAs and viewed along the $[00\bar{1}]$ direction. The TbAs concentration of the layer was approximately 1.8%, and the average particle diameter was approximately 1.5 nm. (b) The rocksalt crystal structure of TbAs and continuous As sublattice throughout the sample are visible. TbAs appears bright in the images.

tric materials. Additionally, TbAs-containing materials are expected to be useful for photoconductive switches and other terahertz applications.

ACKNOWLEDGMENTS

The authors gratefully acknowledge Leszek Wielunski and Ritvik Mathur (Rutgers University) for their generous assistance with RBS measurements and interpretation. This project is funded by the Nanostructured Materials for Power program (DARPA-DSO) with additional support from the National Science Foundation Solar Hydrogen IGERT at the University of Delaware and at UCSB by the National Science Foundation through the UCSB MRL (Award No. DMR 05-20415) and the (U.S.) Army Research Office (Award No. W911NF-0701-0547).

[1]M. Hanson, S. Bank, J. Zide, J. Zimmerman, and A. Gossard, J. Cryst. Growth **301–302**, 4 (2007).
[2]D. C. Driscoll, M. Hanson, C. Kadow, and A. C. Gossard, Appl. Phys. Lett. **78**, 1703 (2001).
[3]C. Kadow, S. B. Fleischer, J. P. Ibbetson, J. E. Bowers, and A. C. Gossard, Appl. Phys. Lett. **75**, 3548 (1999).
[4]D. G. Cahill, W. K. Ford, K. E. Goodson, G. D. Mahan, A. Majumdar, H. J. Maris, R. Merlin, and S. R. Phillpot, J. Appl. Phys. **93**, 793 (2003).
[5]J. M. Zide, D. O. Klenov, S. Stemmer, A. C. Gossard, G. Zeng, J. E. Bowers, D. Vashaee, and A. Shakouri, Appl. Phys. Lett. **87**, 112102 (2005).
[6]P. Pohl *et al.*, Appl. Phys. Lett. **83**, 4035 (2003).
[7]F. J. DiSalvo, Science **285**, 703 (1999).
[8]J. Zide, D. Vashaee, Z. Bian, G. Zeng, J. Bowers, A. Shakouri, and A. Gossard, Phys. Rev. B **74**, 205335 (2006).
[9]K. A. Gschneidner, Jr. and F. W. Calderwood, J. Phase Equilib. **7**, 351 (1986).
[10]J. Bardeen and W. Shockley, Phys. Rev. **80**, 72 (1950).
[11]K. Delaney, N. Spaldin, and C. Van de Walle, Phys. Rev. B **77**, 235117 (2008).
[12]W. R. L. Lambrecht and B. Segall, Phys. Rev. B **41**, 8353 (1990).
[13]L. H. Brixner, J. Inorg. Nucl. Chem. **15**, 199 (1960).
[14]K. E. Singer, P. Rutter, A. R. Peaker, and A. C. Wright, Appl. Phys. Lett. **64**, 707 (1994).
[15]D. O. Klenov, J. M. O. Zide, J. M. LeBeau, A. C. Gossard, and S. Stemmer, Appl. Phys. Lett. **90**, 121917 (2007).
[16]S. Dilhaire, J. M. Rampnoux, S. Grauby, G. Pernot, and G. Calbris, Proceedings of the ASME Micro/Nanoscale Heat and Mass Transfer International Conference, 2009 (unpublished).
[17]M. A. Scarpulla, J. M. O. Zide, J. M. LeBeau, C. G. Van de Walle, A. C. Gossard, and K. T. Delaney, Appl. Phys. Lett. **92**, 173116 (2008).
[18]A. R. Denton and N. W. Ashcroft, Phys. Rev. A **43**, 3161 (1991).
[19]M. A. Scarpulla, T. E. Buehl, B. Mellot, R. V. Chopdekar, K. M. Yu, R. Farshchi, and A. C. Gossard, Presentation at North American Molecular Beam Epitaxy Conference, Breckenridge, CO, 2010 (unpublished).
[20]J. B. Mullin, B. W. Straughan, C. M. H. Driscoll, and A. F. W. Willoughby, J. Appl. Phys. **47**, 2584 (1976).
[21]P. D. Maycock, Solid-State Electron. **10**, 161 (1967).
[22]W. Jones and N. H. March, *Theoretical Solid State Physics* (Courier Dover, New York, 1985).
[23]I. Poole, K. E. Singer, and A. R. Peaker, J. Cryst. Growth **121**, 121 (1992).